

# Fabrication of lightweight, flexible polyetherimide/nickel composite foam with electromagnetic interference shielding effectiveness reaching 103 dB

Wentao Zhai<sup>1</sup>, Yuejuan Chen<sup>1</sup>,  
Jianqiang Ling<sup>1</sup>, Bianying Wen<sup>2</sup> and  
Young-Wook Kim<sup>3</sup>

## Abstract

The preparation of lightweight materials with electromagnetic interference-shielding effectiveness higher than 30 dB is critical for most industrial and consumer applications. Compounding polymer resin with conductive filler can generate excellent electromagnetic interference-shielding effectiveness but usually leads to a high-sample density, while the foaming of polymer composite suffers from the significant-reduced electromagnetic interference-shielding effectiveness. In this study, polyetherimide composite foams with loading of 10–80 phr (parts per hundred of resins) nickel particles were fabricated to meet the gap. The polyetherimide/nickel composite foams possessed uniform cell structure and low-sample density such as 0.86 g/cm<sup>3</sup> at 70 phr nickel. The coupling effects of gravity settlement and cell-structure solidification led to the formation of gradient distribution of nickel particles across the foams. The formed novel structure facilitated the enhancement of multi-reflection and multi-scattering among nickel particles and cells. As a consequence, polyetherimide/nickel foam with 70 phr nickel (PEIN70) possessed a high-electromagnetic interference shielding effectiveness of 86.7–106.5 dB over a frequency range of 50–3000

<sup>1</sup>Ningbo Institute of Material Technology and Engineering, Chinese Academy of Sciences, Zhejiang Province, China

<sup>2</sup>School of Materials and Mechanical Engineering, Beijing Technology and Business University, Beijing, China

<sup>3</sup>University of Seoul, 90 Jeonnon-dong, Dongdaemoon-ku, Seoul, Republic of Korea

## Corresponding author:

Wentao Zhai, Ningbo Institute of Material Technology and Engineering, Chinese Academy of Sciences, Ningbo, Zhejiang Province, 315201, China.

Email: wtzhai@nimte.ac.cn

MHz. When the sample density was considered, the specific electromagnetic interference shielding effectiveness of PEIN70 foam was as high as  $121.3 \text{ dB}/(\text{g}/\text{cm}^3)$  at 1 GHz, which was higher than the reported electromagnetic interference-shielding materials. The excellent electromagnetic interference-shielding properties, lightweight, well-defined resin properties ensure polyetherimide/nickel composite foams useful in many advanced applications.

## Keywords

Polyimide, foam, electrical properties, magnetic properties, electromagnetic interference shielding

## Introduction

Electromagnetic interference (EMI) shielding of radio frequency radiation continues to be a serious concern with extensive applications of sensitive electronic devices and densely packed system. The malfunction of electronics can be harmful for electrical equipments even for human health, as the electronics can be associated with strategic systems such as aircraft, nuclear reactors, and communication systems. EMI shielding is defined as the prevention of the propagation of electric and magnetic waves from one region to another by using conducting or magnetic materials. The shielding can be achieved by minimizing the signal passing through a system either by reflection or absorption of the wave.<sup>1</sup> Nowadays, the preparation of EMI-shielding materials has obtained an increased attention in the academic and industrial fields.

Metals are by far the most common materials for EMI shielding due to their high-electrical conductivity.<sup>2</sup> Polymer/metal composites are attractive for EMI shielding owing to their good moldability. Meanwhile, the dense structure of composites also facilitates to reducing the formation of seams that was commonly encountered in the case of metal sheets,<sup>2</sup> which eliminates the leakage of the radiation. Polymer/metal composites usually exhibit excellent EMI-shielding properties. For example, polyether-sulfone (PES)/nickel (Ni) filament composite with 7 vol% loading has an EMI-shielding effectiveness (SE) of 87 dB at 1 GHz.<sup>3</sup> This value is much higher than those of polymer/carbon-based composites such as 46 dB at 1 GHz for composite with 20 vol% carbon fibers,<sup>4</sup> 60 dB at 1 GHz for composite with 50 wt% carbon nanotube,<sup>5</sup> 47 dB at 1 GHz for composites with carbon nanotube coated with a conducting polymer,<sup>6</sup> and 18 dB at 1–8 GHz for composite with 5 wt% graphene.<sup>7</sup> However, one demerit of metals and polymer/metal composites is their high density.<sup>2,8,9</sup> Therefore, it is desirable to fabricate lightweight polymer/metal composites for the applications of EMI shielding.

Foaming is the most effective approach to reduce the weight of samples for EMI shielding, which is essential in some applications such as aircraft and telecommunication technologies.<sup>10</sup> Yang et al.<sup>10,11</sup> were the first to report on such systems based on polystyrene (PS) foams filled with carbon nanofibers and carbon nanotubes. After that, many researchers reported their investigations on the EMI shielding of polymer composites foams, and the carbon-based materials such as carbon black,<sup>12</sup> carbon fiber,<sup>13–15</sup> carbon nanotube,<sup>16–19</sup> and graphene<sup>7,20–25</sup> were often selected as the conductive fillers. These studies demonstrate that even if the

conductive fillers are diluted in volume due to the foaming, the local concentration of fillers within the cell walls of the foams is comparable with that of the unfoamed counterpart.<sup>21,24</sup> Even in some situation, the local concentration of fillers in foams is higher than that of the latter because of the improved dispersion of fillers during the foaming,<sup>26,27</sup> resulting in increased specific EMI SE.<sup>23</sup> On the other hand, the presence of air inside the materials decreases the permittivity of real parts, while it is also benefit for improving the EMI shielding of materials.

Currently, the used polymer resin of composite foams for EMI shielding is the general plastics such as PS,<sup>10,11</sup> polycaprolactone,<sup>16</sup> polypropylene (PP),<sup>13–15</sup> and poly(methyl methacrylate).<sup>21</sup> The general properties of these polymers, i.e. low heat-resistance, poor flame-retardant properties, and high-smoke generation, restrict their use as the EMI-shielding materials in aerospace and other special fields. Polyetherimide (PEI) is a kind of high-performance polymer with a high  $T_g$  of 215°C, excellent flame retardancy, radiation resistance, and outstanding mechanical properties, which could meet the stringent requirements for specialized applications. However, the high-melt processing temperature of about 340–360°C, high stiffness of polymer matrix, and extremely long gas-saturation time hinder the fabrication of lightweight PEI composite foams,<sup>28–30</sup> especially at high-filler content.

In our previous study, the water vapor-induced phase separation (WVIPS) process had been used to prepare PEI/graphene nanocomposite foams.<sup>24,25</sup> The obtained PEI/graphene foam with 10 wt% graphene loading had a density of 0.29 g/cm<sup>3</sup> and the EMI SE of 10–12 dB at 8–12 GHz. This data is much less than the acceptable value, i.e. 30 dB, for most industrial and consumer applications. The main target of this study is to fabricate lightweight PEI composite foams with the EMI SE higher than 30 dB. Ni particles with superior oxidation resistance were selected as the conductive filler, and the WVIPS method was used to fabricate PEI/Ni composite foams. The gradient distribution of Ni particles was generated at the cross section of foams due to the coupling effects of cell-structure solidification and gravity settlement of Ni particles. The influences of gradient distribution of Ni particles on the electrical conductivity and EMI shielding properties of PEI/Ni composite foams were investigated. It was found that the EMI SE of PEI/Ni foam with the density of 0.86 g/cm<sup>3</sup> was about 103 dB at 1 GHz, which is much higher than the EMI SE value of the reported polymer composites with the density higher than 1.00 g/cm<sup>3</sup>. The excellent EMI-shielding properties, lightweight, and well-defined resin properties ensure PEI/Ni composite foams' potential use in many advanced fields.

## Experimental

### Materials

PEI (Ultem1000) was obtained from General Electrical Company, which is transparent amber-colored particle with a density of 1.28 g/cm<sup>3</sup>, and the glass transition temperature ( $T_g$ ) is 215°C. Raw commercial Ni powder was purchased from Zhongnuo Advanced Material Technology Co. Ltd, China, with the particle size

of 1–3  $\mu\text{m}$ , purity of 98%, and density of 8.90 g/cm<sup>3</sup>. *N,N*-Dimethyl formamide (DMF) was supplied by Sinopharm Chemical Reagent (China) and used as received.

### *Preparation of microcellular PEI/Ni composites foams*

A WVIPS process was carried out to prepare microcellular PEI/Ni composites foams.<sup>23</sup> PEI and Ni were solution blended with vigorous stirring for 5 h at 100°C using DMF as the solvent. The resultant dispersion of PEI/Ni/DMF was poured on a glass plate and then exposed in air with a humidity of 75% and temperature of 25°C. The obtained foam sheets were immersed in cold water to remove the residual DMF and then were dried at 180°C for 36 h to remove the residual water and DMF. A series of PEI/Ni composites foams with Ni content of 10, 20, 30, 40, 50, 60, 70, and 80 phr (parts per hundred of resins) obtained were hereafter coded as PEIN10, PEIN20, PEIN30, PEIN40, PEIN50, PEIN60, PEIN70, and PEIN80 foams, respectively.

### *Characterizations*

The densities of microcellular PEI/Ni foams ( $\rho_f$ ) were measured via the water-displacement method in accordance with ASTM D792.

The cell morphology and the dispersion of Ni were observed by using Hitachi TM-1000 scanning electric microscope (SEM). The samples were freeze-fractured in liquid nitrogen and sputter-coated with platinum for 90 s.

The surface electrical conductivity of the moderately conductive samples ( $>1 \times 10^{-8}$  S/cm) was measured using Solartron 1287 electrochemical workstation (Advanced Measurement Technology Inc. USA). The samples with conductivity lower than  $1 \times 10^{-8}$  S/cm were measured with three-terminal fixture on an EST121 ultrahigh resistance and micro current meter (Beijing EST Science & Technology Co. Ltd.) according to ASTM D257. Circular plates with a diameter of 7 cm were cut for conductivity measurement, and the sputter-coating treatment was carried out to reduce the contact resistance between the electrodes and the sample.

Magnetic characterizations of microcellular PEIN composites foams were performed using physical property measurement system (PPMS) by Quantum Design at 25°C.

The EMI SE of microcellular PEI/Ni composite foams at the frequency of 50 MHz–1.5 GHz was studied by applying a DR-S02 coaxial SE test instrument (Beijing Dingrong Science & Technology Co. Ltd.) according to ASTM D4935-2010. The test data were extended to 3 GHz by a NA7300 vector network analyzer (Tianjin Deviser Electronics Instrument Co. Ltd.). The thickness of specimens was about 1.8 mm.

## **Results and discussion**

### *Preparation and characterizations of PEIN composite foams*

A WVIPS process was used to prepare PEIN composite foam. The typical optical micrographs of PEIN70 composite foam with 70 phr Ni are indicated in Figure 1(a).

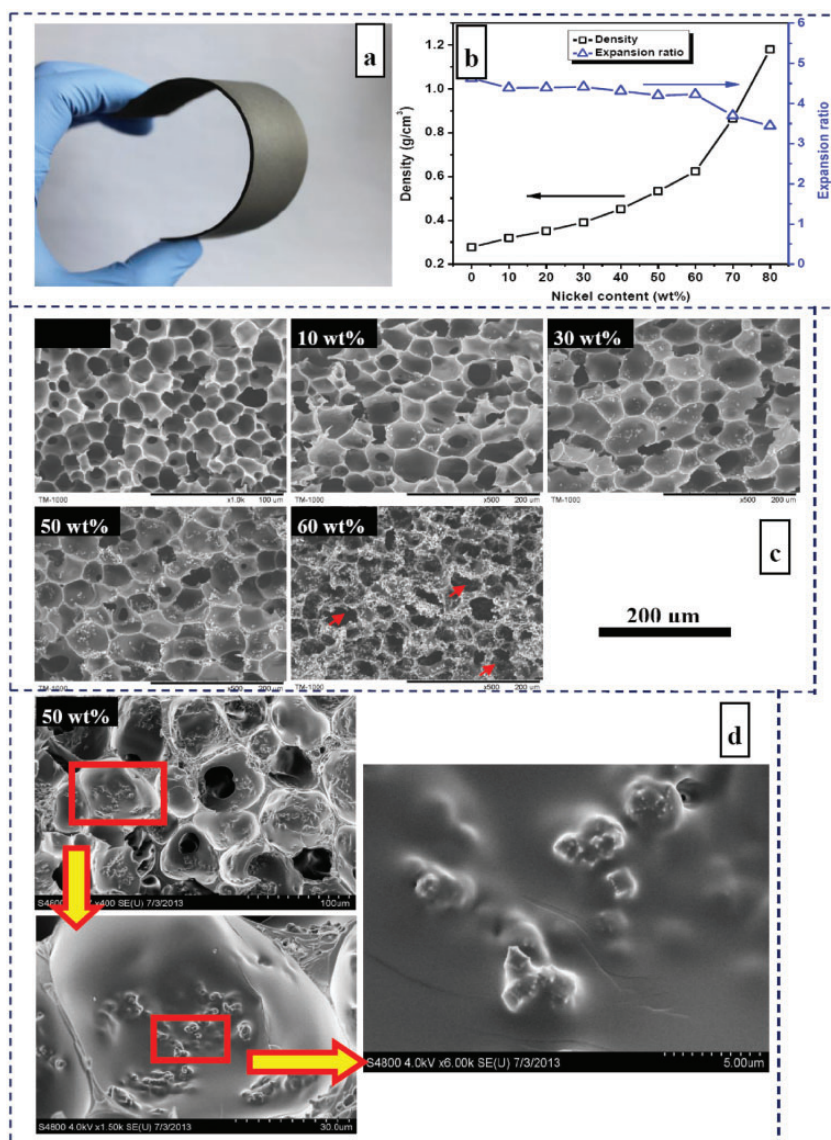


**Figure 1.** Photograph (a), density (b), expansion ratio (b), and SEM micrographs (c) of PEIN composite foams, and SEM micrographs illustrating the dispersion of Ni particles in PEIN50 foam (d).

The thickness of foam sheet was 1.8 mm, and it was quite flexible under bending. Figure 1(b) summarizes the densities and expansion ratio of PEIN composite foams as a function of Ni content. PEI foam had a density of  $0.28 \text{ g/cm}^3$  and expansion ratio of 4.6. With the introduction of Ni particles, however, the density of PEIN

composite foams increased gradually up to  $0.32 \text{ g/cm}^3$  for PEIN10 foam,  $0.35 \text{ g/cm}^3$  for PEIN20 foam,  $0.39 \text{ g/cm}^3$  for PEIN30 foam,  $0.45 \text{ g/cm}^3$  for PEIN40 foam,  $0.53 \text{ g/cm}^3$  for PEIN50 foam, and  $0.62 \text{ g/cm}^3$  for PEIN60 foam, respectively; while no obvious change in expansion ratio, i.e. 4.3, was observed. This phenomenon suggested that the introduction of Ni particles did not affect the foaming behavior of PEI obviously, and the increased density of PEIN composite foams was only attributed to the increased concentration of Ni particle. As mentioned above, Ni particle has a much higher density in relative to PEI resin, i.e.  $8.90 \text{ vs } 1.28 \text{ g/cm}^3$ . At higher Ni content, the as-prepared PEIN composite foams exhibited the increased density and the decreased expansion ratio, which indicated that a high loading of Ni might spoil the cell structure of PEIN composite foam.

Figure 1(c) shows the SEM micrographs of PEIN composite foams. PEI foam presented the polygonal-cell structure with the size of  $42.5 \mu\text{m}$  and uniform cell-structure distribution. With the addition of Ni particles, the well-defined cell structure was kept in PEIN composite foams but its cell size tended to increase slightly. In addition, the Ni particles were located on the cell walls, and its concentration among the cells increased gradually with the Ni content. At higher Ni loading of 70 phr, the Ni particles covered up the cell structure, and the obvious cell-coalescence phenomenon occurred as pointed by the red arrows.

SEM micrographs with higher magnifications were used to figure out the dispersion of Ni particles among the cells and the compatibility of Ni particles with PEI matrix. As indicated in Figure 1(d), the Ni particles were dispersed both on the cell walls and the cell struts. At higher SEM magnification, it seems that most of the Ni particles were not exposed in air but was covered by the polymer film. Moreover, the Ni particles with the size of  $1\text{--}3 \mu\text{m}$  were dispersed among the cells separately.

The used Ni particles in this study were not modified, and the inert surface of Ni particles cannot offer any chemical interaction with the PEI matrix. Therefore, the foaming process might be the reason for the improved dispersion of Ni particles even at high loading.<sup>26,27</sup> It is well accepted that the cell nucleation prefers to take place at polymer/filler interfaces owing to the reduced energy barrier for heterogeneous nucleation in relative to homogeneous nucleation.<sup>31</sup> With the diffusion of water vapor into dispersion and the diffusion of DMF into air, the phase separation occurred and the nuclei took place.<sup>32</sup> The cell-growth process is an extensional flow of polymer solution in nature.<sup>33</sup> Our previous study verified that the in situ-formed strain rate was as high as  $20\text{--}130 \text{ s}^{-1}$  during the cell growth.<sup>34</sup> This strong-stretching action tended to push the surrounded dispersion, and the generated force was then transferred from matrix onto Ni particles, which process improved the dispersion of Ni particles and enriched the Ni particles on cell walls. The improved dispersion of nanoparticles in polymer matrix due to foaming had been observed in PC/silica and PP/silica-foaming systems.<sup>26,27</sup> More interestingly, we found that the foaming process facilitated the orientation of graphene nanosheets around cell wall in PEI/graphene-foaming system.<sup>23</sup>



### *Gradient distribution of Ni particles in PEIN composite foams*

Compared to PEI/DMF solution, the Ni particle has higher density. During the foaming process, the Ni particles tended to precipitate under the action of gravity. Considering the precipitation process of Ni particles was accompanying with the solidification of cell structure, the Ni particles might present a vertical gradient distribution in the foams. The dispersion of Ni particles was investigated by SEM micrographs of the whole cross section of PEIN60 foam. As indicated in Figure 2(a), the Ni particles were dispersed in the cells. It seems that the concentration of Ni particle at the top of cells was lower than that at the bottom of cells. The representative SEM micrographs of the upper and lower surfaces of PEIN60 foam are presented in Figure 2(b) and (c), respectively, with the aim to further demonstrate the formation of gradient distribution. It is seen that a small amount of Ni particles aggregates was randomly dispersed on the upper surface of PEIN60 foam. In the case of the lower surface, however, most of matrix was covered by the Ni particles. These results verified that the coupling effects of cell-structure solidification and gravity settlement allowed the formation of the gradient distribution of Ni particles in the foams.

In addition to the gradient distribution of Ni particles, the cell-structure size also exhibited a gradient distribution in the cross-section of the foam. As indicated in Figure 2(a), the smaller cell size and higher cell density were observed near the upper surface while the larger cell size and lower cell density were seen near the lower surface. In the foaming process of PEIN solution, the cell nucleation and growth processes were along with the phase-separation process. The cell-growth rate was determined by the double-diffusion rates of DMF and water vapor. The upper surface of PEIN solution was contact with air, a shorter cell growth time was needed and thus led to the formation of smaller cell size.<sup>32</sup> Compared to the upper surface, a longer double-diffusion time or cell growth time was required for the lower surface of solution, because the water vapor took a longer time to diffuse into the bottom of PEIN solution, resulting in the formation of larger cell size.

### *Surface conductivity and magnetic properties of PEIN composite foams*

It is well accepted that the dielectric and magnetic losses are the main mechanism to determine the EMI SE of materials. The electrical conductivity and magnetic properties of PEIN composite foams were investigated, and the results are shown in Figure 3(a) and (b), respectively. As indicated in Figure 3(a), PEI foam was one kind of electric-insulating material with a surface electrical conductivity of  $\sim 2.95 \times 10^{-14}$  S/cm. With the addition of Ni particles, the obtained PEIN composite foams exhibited an increased electrical conductivity but with the different tendency at their upper and lower surfaces, resulting from the gradient distribution of Ni particles across the foams. For the upper surface, the electrical conductivity of foams increased slightly up to  $6.19 \times 10^{-12}$  S/cm at the Ni content of 40 phr. For the lower surface, however, the electrical conductivity of foams reached  $2.25 \times 10^{-6}$  S/cm at the Ni content of 20 phr. At higher Ni loading, the electrical

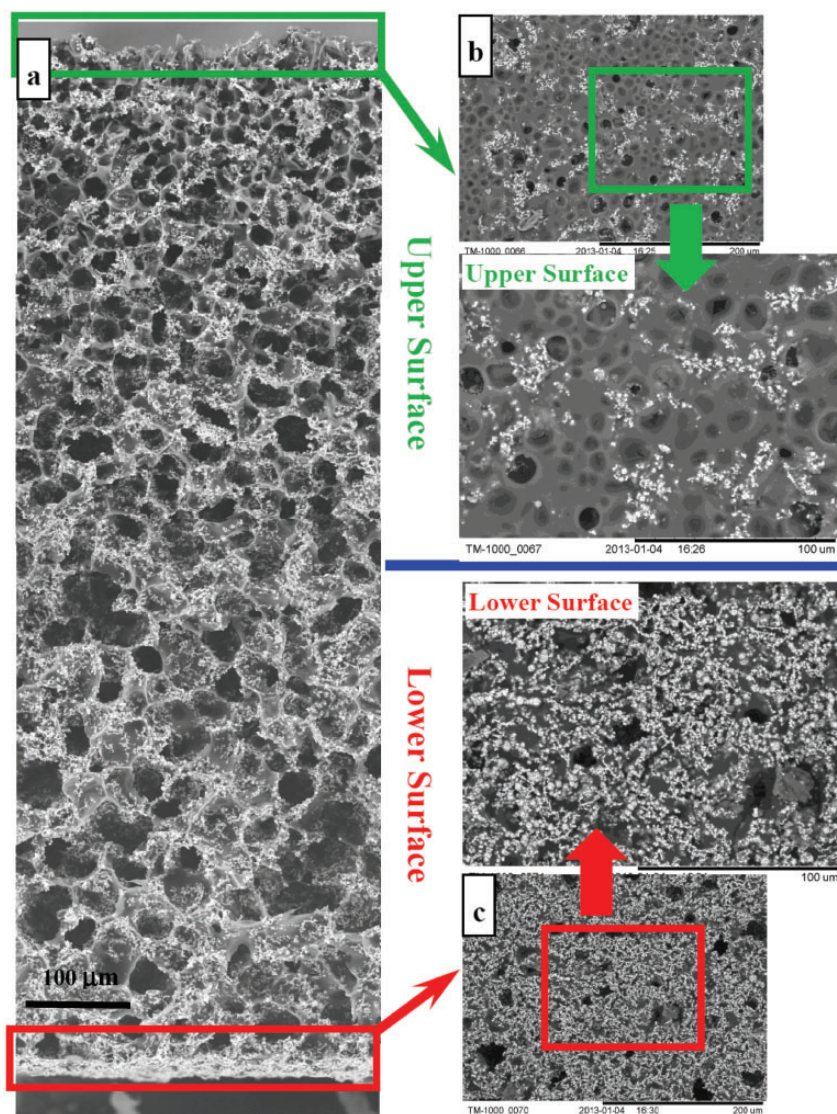


**Figure 2.** The vertical-gradient distribution of Ni particles along the cross section of PEIN60 composite foam.

conductivity of the two surfaces increased gradually to the equilibrium value of about  $1.32 \times 10^{-2}$  and  $1.98 \times 10^{-2}$  S/cm, respectively. It is seen that the upper and lower surfaces presented the large difference in the electrical conductivity of seven to nine orders of magnitude at the Ni content of 20–40 wt%, and this difference significantly reduced at higher Ni loading. These results further verified the formation of gradient distribution of Ni particles across the foam.



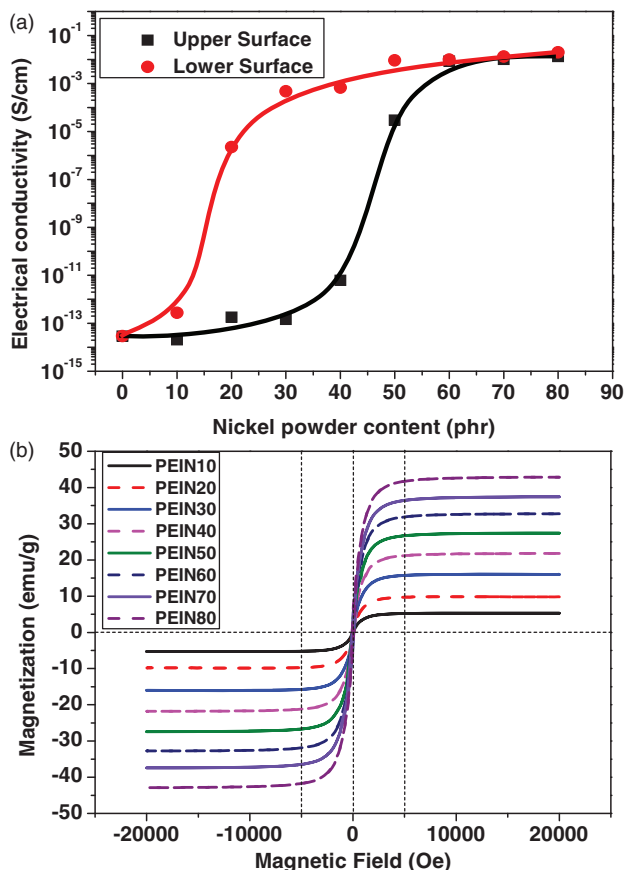


**Figure 3.** The surface electrical conductivity of the upper and lower surfaces of PEIN composite foams as a function of Ni content (a) and magnetization curves of PEIN composite foams (b).

The magnetic properties of the as-prepared PEIN composite foams were measured by VSM, and the magnetic hysteresis curve of samples was plotted in Figure 3(b). It is seen that PEIN composite foams were ferromagnetic, and the magnetization could saturate at the magnetic field of about 5.0 kOe. PEIN10 foam had a saturation magnetization ( $M_s$ ) of 5.06 emu/g. The increase in Ni loading tended to linearly increase the  $M_s$ . As for PEIN80 foam, its  $M_s$  was about 42.45 emu/g.

### *The EMI SE of microcellular PEIN composite foams*

The EMI SE of PEIN composite foams with the thickness of 1.8 mm was measured at 50–3000 MHz. As shown in Figure 4(a), the EMI SE of all the foams exhibited weak frequency dependency in the measured frequency region. The EMI SE of PEIN10 foam was 18.0–25.7 dB over a frequency range of 50–3000 MHz. With the increase of Ni content, the EMI SE of PEIN foams increased gradually up to 36.8–41.2 dB for

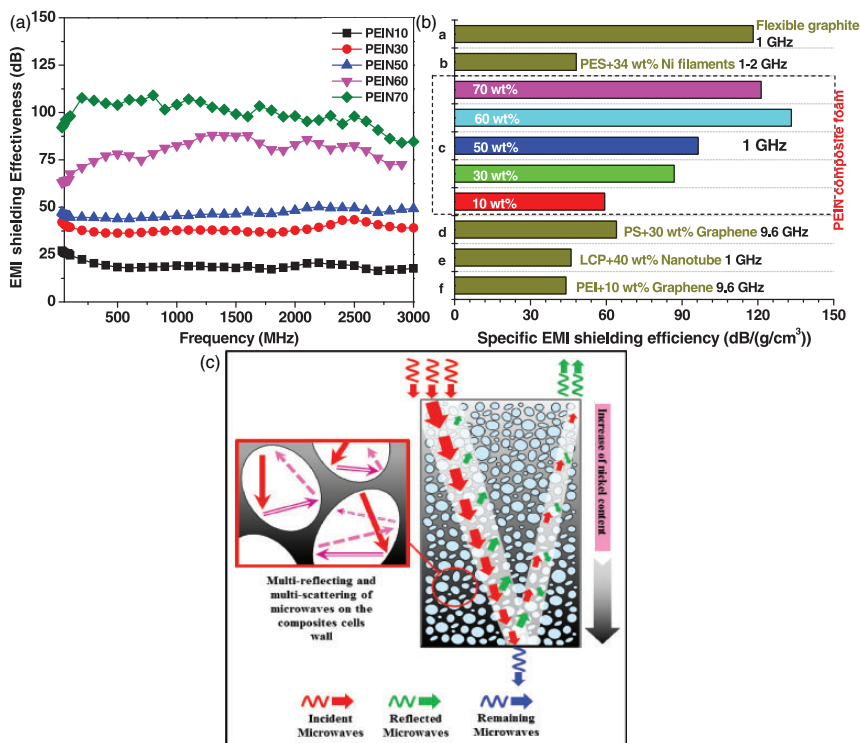


**Figure 4.** The EMI SE of PEIN composite foams as 50–3000 Hz (A). Comparison of specific EMI SE of our data with other reported results: (a) obtained from Luo et al.;<sup>32</sup> (b) obtained from Shui and Chuang;<sup>3</sup> (c) in this study; (d) obtained from Fletcher et al.;<sup>17</sup> (e) obtained from Jou et al.;<sup>5</sup> and (f) obtained from Yan et al.<sup>20</sup> (B). The schematic description of the effects of gradient structure on the incident microwaves (C).

PEIN30 foam, 44.7–50.2 dB for PEIN50 foam, 64.0–82.4 dB for PEIN60 foam, and 86.7–106.5 dB for PEIN70 foam, respectively. These results indicated that the EMI SE of the foams increased with the increase in Ni content.

The lightweight design for EMI-shielding materials is essential in some applications such as aircraft and telecommunication technologies. The specific EMI SE, which represents the material-utilizing efficiency, was calculated on the basis of the rate of total EMI SE and the sample density.<sup>23</sup> As shown in Figure 4(b), the specific EMI SE of PEIN foams at 1 GHz was about 59.3 dB/(g/cm<sup>3</sup>) for PEIN10 foam. With further increase in the Ni content, the specific of samples reached 86.9 dB/(g/cm<sup>3</sup>) for PEIN30 foam and 96.3 dB/(g/cm<sup>3</sup>) for PEIN50 foam. At the Ni particle loading of 60 wt%, the maximum specific EMI SE of 133.2 dB/(g/cm<sup>3</sup>) was obtained in PEIN60 foam. At higher Ni content, the specific EMI SE of PEIN70 foam decreased slightly to 121.3 dB/(g/cm<sup>3</sup>). This suggested that too much Ni particles loading might decrease the specific EMI SE of PEIN foams, due to the formation of poor cell structure as shown in Figure 2.

**Table 1.** The thickness of samples indicated in references.

References	a	b	c	d	e	f
	32	3	This study	17	5	20
Thickness of sample (mm)	3.1	2.8	1.8	2.5	1.0	1.8

Figure 4(b) summarizes the comparative data of the specific EMI SE of this work with other studies, and Table 1 shows the thickness of samples mentioned in references. As reported, PES/Ni filament composite with 7 vol% (34 wt%) loading had a high-EMI SE of 87 dB at 1 GHz.<sup>3</sup> This value was much higher 45.6 dB at 1 GHz of PEIN30 foam with 30 phr Ni particle loading in this study. It is believed that the volume expansion and the shorter aspect ratio of Ni particles in relative to Ni filament were the possible reason behind the phenomenon. When the sample density was carried in, however, the specific SE of PEIN30 foam was about 86.9 dB/(g/cm<sup>3</sup>) while that of PES/Ni filament was only about 48.1 dB/(g/cm<sup>3</sup>). The use of carbon-based materials for EMI shielding is very popular because of their low density. A high-EMI SE value of 60 dB at 1 GHz was obtained by Jou et al.<sup>5</sup> in LCP nanocomposites with loading of 40 wt% nanotube. A similar data were achieved at PEIN60 foam in this study. As the value of the EMI SE was divided by the sample density, however, the specific EMI SE of the former was much lower than that of the later, i.e.  $\sim 46.0$  vs 133.2 dB/(g/cm<sup>3</sup>). The EMI SE of flexible graphite, made by the compression of exfoliated graphite in the absence of a binder, reaches 130 dB at 1 GHz, which is higher than or comparable to all the reported EMI-shielding materials.<sup>35</sup> The density of flexible graphite is 1.1 g/cm<sup>3</sup>, and the calculated specific EMI SE is about 118.1 dB/(g/cm<sup>3</sup>). This value was lower than 133.2 dB/(g/cm<sup>3</sup>) for PEIN60 foam and 121.3 dB/(g/cm<sup>3</sup>) for PEIN70 foam, because the PEIN foams had much lower density than the flexible graphite, i.e. 0.62 and 0.86 vs 1.1 g/cm<sup>3</sup>. These results fully demonstrated that the foaming process was very efficient in preparing PEIN composite foams with lightweight and excellent EMI-shielding properties.

In general, the EMI SE of material ( $SE_{total}$ ) includes the contribution of absorption ( $SE_A$ ), reflection ( $SE_R$ ), and multiple internal reflections ( $SE_M$ ). Table 2 summarizes the influences of foaming on the specific EMI SE of PEIN and the  $SE_A/SE_{total}$ . It is seen that PEIN composites and PEIN composites foams presented the similar specific EMI SE, and the reflection was the main mechanism for EMI shielding. Furthermore, it is interesting to find that the  $SE_A/SE_{total}$  of PEIN composites increased from 0% up to 20.2–25.1%. This indicated that the presence of cellular structures enhanced the absorption of the electromagnetic waves.

The complex structure design has been used to improve the shielding performances of materials. Foaming is one important strategy for structure design. Besides the weight reduction, foaming can supply a large amount of well-dispersed air in polymer matrix, which decreases the permittivity of real parts and, thereafter, decreases the microwave reflectivity at the material surface. The generation of multilayered structure is another strategy to further improve the EMI-shielding

**Table 2.** The specific  $SE_{total}$  and the  $SE_A/SE_{total}$  of PEIN composites before and after foaming.

	PEIN10	PEIN30	PEIN50	PEIN60	PEIN70
<i>Concentration</i>					
Phr	10	30	50	60	70
wt%	9.1	23.1	33.3	37.5	41.2
The specific $SE_{total}$ of composites	64.0 dB/(g/cm <sup>3</sup> )	84.1 dB/(g/cm <sup>3</sup> )	92.7 dB/(g/cm <sup>3</sup> )	127.5 dB/(g/cm <sup>3</sup> )	119.2 dB/(g/cm <sup>3</sup> )
The specific $SE_{total}$ of composites foams	59.3 dB/(g/cm <sup>3</sup> )	86.9 dB/(g/cm <sup>3</sup> )	96.3 dB/(g/cm <sup>3</sup> )	133.2 dB/(g/cm <sup>3</sup> )	121.3 dB/(g/cm <sup>3</sup> )
$SE_A/SE_{total}$ for composites	~0%	~0%	~0%	~0%	~0%
$SE_A/SE_{total}$ for composites foams	~25.1%	~20.9%	~22.1%	~21.8%	~20.2%

properties of materials.<sup>36</sup> The multi-reflection formed among layers facilitates the dissipation.<sup>37</sup> These multilayered structures could reduce the skin effect and enhance the absorption properties materials by the multi-reflection and multi-scattering. It seems that the prepared PEIN foam in this study included the two strategies. As indicated in Figure 4(c), the gradient concentration of Ni particles across cell walls provided a multilayered structure, which tended to enhance the absorption of electromagnetic wave as indicated in Table 2.

## Conclusions

In this study, the WVIPS process was carried out to fabricate PEI/Ni composite foams. The pure PEI foam exhibited uniform-cell distribution and high-expansion ratio of 4.6. The addition of Ni particles increased the cell size of PEIN foam slightly. On the other hand, the presence of Ni particles increased the foam density gradually but did not change the expansion ratio of PEIN foams. At higher Ni contents of 70 and 80 phr, PEIN foams showed the reduced expansion ratio due to the occurrence of cell coalescence. Ni particles have a much higher density than that of PEI solution, which lead to the precipitation of Ni particles under gravity during the solidification process of cell structure. The coupling effects of gravity settlement and cell-structure solidification induced the formation of gradient distribution of Ni particles across the foams. The presence of gradient distribution of Ni particles enhanced the multi-reflection and multi-scattering, which endowed with PEIN composite foams with excellent-specific EMI SE.

## Funding

The authors are grateful to the National Natural Science Foundation of China (grants 51003115, 21274007), and Ningbo Natural Science Foundation (grant no. 2011A6101118) for their financial support of this study.

## Conflict of interest

The authors declared no potential conflicts of interest with respect to the research, authorship, and/or publication of this article.

## References

1. Tong XC. *Advanced materials and design for electromagnetic interference shielding*. London: CRC Press Taylor & Francis Group, 2009.
2. Chung DDL. Electromagnetic interference shielding effectiveness of carbon materials. *Carbon* 2001; 39: 279–285.
3. Shui X and Chuang DDL. Nickel filament polymer-matrix composites with low surface impedance and high electromagnetic interference shielding effectiveness. *J Electron Mater* 1997; 26: 928–934.
4. Li L and Chuang DDL. Electrical and mechanical properties of electrically conductive polyethersulfone composite. *Composities* 1994; 25: 215–224.
5. Jou W, Cheng H and Hsu C. The electromagnetic shielding effectiveness of carbon nanotubes polymer composites. *J Alloys Compounds* 2007; 434–435: 641–645.
6. Yuan J, Im JS, Kim H, et al. Effect of oxyfluorination on electromagnetic interference shielding of polyaniline-coated multi-walled carbon nanotubes. *Colloid Polym Sci* 2011; 289: 1749–1755.
7. Eswaraiah V, Sankaranarayanan V and Ramaprabhu S. Functionalized graphene-PVDF foam composites for EMI shielding. *Macromol Mater Eng* 2011; 296: 894–898.
8. Chuang DDL. Carbon materials for structural self-sensing, electromagnetic shielding and thermal interfacing. *Carbon* 2012; 50: 3342–3353.
9. Thomassin JM, Jérôme C, Pardoën T, et al. Polymer/carbon based composites as electromagnetic interference (EMI) shielding materials. *Mater Sci Eng R Rep* 2013; 74: 211–232.
10. Yang Y, Gupta MC, Dudley KL, et al. Conductive carbon nanofiber polymer foam structures. *Adv Mater* 2005; 17: 1999–2003.
11. Yang Y, Gupta MC, Dudley KL, et al. Novel carbon nanotube-polystyrene foam composites for electromagnetic interference shielding. *Nano Lett* 2005; 5: 2131–2134.
12. Mahapatra S, Sridhar V and Tripathy DK. Impedance analysis and electromagnetic interference shielding effectiveness of conductive carbon black reinforced microcellular EPDM rubber vulcanizates. *Polym Compos* 2008; 29: 465–472.
13. Ameli A, Jung PU and Park CB. Through-plane electrical conductivity of injection-molded polypropylene/carbon-fiber composite foams. *Compos Sci Technol* 2013; 76: 37–44.
14. Ameli A, Jung PU and Park CB. Electrical properties and electromagnetic interference shielding effectiveness of polypropylene/carbon fiber composite foams. *Carbon* 2013; 60: 379–391.
15. Wang CB, Ying S and Xiao Z. Preparation of short carbon fiber/polypropylene fine-celled foams in supercritical CO<sub>2</sub>. *J Cell Plast* 2013; 49: 65–82.
16. Thomassin JM, Pagnouille C, Bednarsz L, et al. Foams of polycaprolactone/MWNT nanocomposites for efficient EMI reduction. *J Mater Chem* 2008; 18: 792–796.
17. Fletcher A, Gupta MC, Dudley KL, et al. Elastomer foam nanocomposites for electromagnetic dissipation and shielding applications. *Compos Sci Technol* 2010; 70: 938–953.
18. Antunes M, Gedler G and Velasco JI. Multifunctional nanocomposite foams based on polypropylene with carbon nanofillers. *J Cell Plast* 2013; 49: 259–279.
19. Ameli A, Nofar M, Park CB, et al. Polypropylene/carbon nanotube nano/microcellular structures with high dielectric permittivity, low dielectric loss, and low percolation threshold. *Carbon* 2014; 71: 206–217.



20. Yan DX, Ren PG, Pang H, et al. Efficient electromagnetic interference shielding of lightweight graphene/polystyrene composite. *J Mater Chem* 2012; 22: 18772–18774.
21. Zhang HB, Yan Q, Zheng WG, et al. Tough graphene-polymer microcellular foams for electromagnetic interference shielding. *ACS Appl Mater Interfaces* 2011; 3: 918–924.
22. Zhu JH, Wei SY, Haldolaarachchige N, et al. Electromagnetic field shielding polyurethane nanocomposites reinforced with core-shell Fe-Silica nanoparticles. *J Phys Chem C* 2011; 115: 15304–15310.
23. Ling JQ, Zhai WT, Feng WW, et al. Facile preparation of lightweight microcellular polyetherimide/graphene composite foams for electromagnetic interference shielding. *ACS Appl Mater Interfaces* 2013; 5: 2677–2684.
24. Shen B, Zhai WT, Tao MM, et al. Lightweight, multifunctional polyetherimide/graphene@Fe<sub>3</sub>O<sub>4</sub> composite foams for shielding of electromagnetic pollution. *ACS Appl Mater Interfaces* 2013; 5: 11383–11391.
25. Shen B, Zhai WT, Lu DD, et al. Fabrication of microcellular polymer/graphene nanocomposite foams. *Polym Int* 2012; 61: 1693–1702.
26. Zhai WT, Yu J, Wu LC, et al. Heterogeneous nucleation uniformizing cell size distribution in microcellular nanocomposites foams. *Polymer* 2006; 47: 7580–7589.
27. Zhai WT, Park CB and Kontopoulou M. Nanosilica addition dramatically improves the cell morphology and expansion ratio of polypropylene heterophasic copolymer foams blown in continuous extrusion. *Ind Eng Chem Res* 2011; 50: 7282–7289.
28. Miller D, Chatchaisucha P and Kumar V. Microcellular and nanocellular solid-state polyetherimide (PEI) foams using sub-critical carbon dioxide I. Processing and structure. *Polymer* 2009; 50: 5576–5584.
29. Miller D and Kumar V. Microcellular and nanocellular solid-state polyetherimide (PEI) foams using sub-critical carbon dioxide II. Tensile and impact properties. *Polymer* 2011; 52: 2910–2919.
30. Zhai WT, Feng WW, Ling JQ, et al. Fabrication of lightweight microcellular polyimide foams with three-dimensional shape by CO<sub>2</sub> foaming and compression molding. *Ind Eng Chem Res* 2012; 51: 12827–12834.
31. Zhai WT, Yu J, Wang HY, et al. Foaming behavior of polypropylene/polystyrene blends enhanced by improved interfacial compatibility. *J Polym Sci, Part B: Polym Phys* 2008; 46: 1641–1651.
32. Park HC, Kim YP, Kim HY, et al. Membrane formation by water vapor induced phase inversion. *J Membr Sci* 1999; 156: 169–178.
33. Zhai WT, Kuboki T, Wang L, et al. Cell structure evolution and the crystallization behavior of polypropylene/clay nanocomposites foams blown in continuous extrusion. *Ind Eng Chem Res* 2010; 49: 9834–9845.
34. Zhai WT, Wang J, Chen N, et al. The orientation of carbon nanotubes in poly(ethylene-co-octene) microcellular foaming and its suppression effect on cell coalescence. *Polym Eng Sci* 2012; 52: 2078–2089.
35. Luo X and Chuang DDL. Electromagnetic interference shielding reaching 130 dB using flexible graphite. *Carbon* 1996; 34: 1293–1294.
36. Yuen SM, Ma CCM, Chuang CY, et al. Effect of processing method on the shielding effectiveness of electromagnetic interference of MWCNT/PMMA composites. *Compos Sci Technol* 2008; 68: 963–968.
37. Chen M, Zhou Y, Pan Y, et al. Gradient multilayer structural design of CNTs/SiO<sub>2</sub> composites for improving microwave absorbing properties. *Mater Des* 2011; 32: 3013–3016.